PHYSICAL REVIEW B **100**, 161112(R) (2019)

Rapid Communications

Unusual Mott transition associated with charge-order melting in $BiNiO_3$ under pressure

I. Leonov,[1,2] A. S. Belozerov,[1,3] and S. L. Skornyakov[1,3]
[1]*M. N. Miheev Institute of Metal Physics, Russian Academy of Sciences, 620108 Yekaterinburg, Russia*
[2]*Materials Modeling and Development Laboratory, National University of Science and Technology "MISiS," 119049 Moscow, Russia*
[3]*Ural Federal University, 620002 Yekaterinburg, Russia*

(Received 5 August 2019; revised manuscript received 9 August 2019; published 28 October 2019)

We study the electronic structure, magnetic state, and phase stability of paramagnetic $BiNiO_3$ near a pressure-induced Mott insulator-to-metal transition (MIT) by employing a combination of density functional and dynamical mean-field theory. We obtain that $BiNiO_3$ exhibits an anomalous negative-charge-transfer insulating state, characterized by charge disproportionation of the Bi 6*s* states, with Ni^{2+} ions. Upon a compression of the lattice volume by ~4.8%, $BiNiO_3$ is found to make a Mott MIT, accompanied by the change of crystal structure from triclinic $P\bar{1}$ to orthorhombic *Pbnm*. The pressure-induced MIT is associated with the melting of charge disproportionation of the Bi ions, caused by a charge transfer between the Bi 6*s* and O 2*p* states. The Ni sites remain to be Ni^{2+} across the MIT, which is incompatible with the valence-skipping Ni^{2+}/Ni^{3+} model. Our results suggest that the pressure-induced change of the crystal structure drives the MIT in $BiNiO_3$.

DOI: 10.1103/PhysRevB.100.161112

The Mott metal-insulator transition driven by correlation effects has been an outstanding problem in condensed-matter physics over many decades [1]. In recent years, increasing attention has been drawn to the rare-earth nickelate perovskites RNiO$_3$ (R = rare earth, R^{3+}) with a high oxidation state of nickel, Ni^{3+} $3d^7$ [2–4]. RNiO$_3$ compounds (except for $LaNiO_3$) exhibit a sharp metal-insulator transition (MIT) upon cooling below T_{MIT} [5]. The phase transition is accompanied by a structural transformation from an orthorhombic (*Pbnm*, $GdFeO_3$-type) to monoclinic ($P2_1/n$) crystal structure, with a cooperative breathing distortion of NiO_6 octahedra [5].

Based on the Ni-O bond lengths analysis and x-ray absorption spectroscopy, a partial $Ni^{(3\pm\delta)+}$ charge disproportionation of Ni ions was proposed to occur in the insulating RNiO$_3$ phases [5,6]. By contrast, further electronic structure calculations explain the insulating state of RNiO$_3$ in terms of bond disproportionation, with alternating Ni ions which (nearly) adopt a Ni^{2+} $3d^8$ (Ni^{2+} ions with local moments) and $3d^8\underline{L}^2$ (nonmagnetic spin-singlet) electronic configuration ($\underline{L}$ denotes a hole in the O 2*p* band) [3,7,8]. The transition temperature T_{MIT} is strongly related to the degree of structural distortion of RNiO$_3$, determined by the size of *R* ions. With decrease of the *R*-ionic radius, the Ni-O-Ni bond angle, which determines the degree of overlapping of the Ni 3*d* and O 2*p* orbitals (and hence the Ni 3*d* bandwidth), becomes smaller and T_{MIT} is increased. In accord with this, the least distorted $LaNiO_3$ is found to be a correlated metal [5,9]. In this context, the replacement of La^{3+} with a larger ion, such as Bi^{3+}, should in principle result in a metal with (nearly) cubic perovskite structure. By contrast, $BiNiO_3$ has been found to be an insulator with a highly distorted perovskite structure (triclinic, $P\bar{1}$) and unusual valence ordering of the *A*-site Bi ions [10]. In particular, based on x-ray and neutron diffraction, it was proposed that Ni ions adopt a Ni^{2+} state, with an electronic configuration $Bi^{3+}_{0.5}Bi^{5+}_{0.5}Ni^{2+}O_3$ [10–12].

$BiNiO_3$ is known due to its colossal negative thermal expansion across the pressure-induced MIT, as suggested caused by a Bi/Ni charge transfer [13]. Under ambient conditions, $BiNiO_3$ crystallizes in a triclinic perovskite crystal structure (space group $P\bar{1}$, a subgroup of $P2_1/n$) with two inequivalent Bi and four Ni sites [11] (see Supplemental Material Fig. S1 [14] and Ref. [15], therein). It is an insulator with an energy gap of 0.68 eV [10]. Below the Néel temperature of $T_N \sim 300$ K, $BiNiO_3$ is a *G*-type antiferromagnet with a near-antiferromagnetic alignment of Ni^{2+} $S = 1$ spins, implying a predominant role of the antiferromagnetic Ni-O-Ni superexchange [10,12,16]. Moreover, similarly to the small *R* ions RNiO$_3$ the (charge-disproportionated) paramagnetic insulating phase of $BiNiO_3$ extends well above T_N, implying the crucial importance of correlation effects [3,7,17]. $BiNiO_3$ shows a Mott insulator-to-metal phase transition (in the paramagnetic phase) under pressure (above ~4 GPa) or upon substitution of the *A*-site Bi ions with La [18,19]. In close similarity to RNiO$_3$, the MIT is accompanied by the change of crystal structure from the triclinic $P\bar{1}$ (insulating) to orthorhombic $GdFeO_3$-type *Pbnm* (metallic) phase, with a volume collapse of ~3% and melting of charge disproportionation (Ni and Bi sites are equivalent in the *Pbnm* structure of $BiNiO_3$). Based on the powder x-ray absorption and neutron diffraction, it was proposed that the melting of charge disproportionation leads to a charge transfer from Ni^{2+} to Bi^{3+}, so that the electronic state of the *Pbnm* metallic phase can be described as $Bi^{3+}Ni^{3+}O_3$ [11,20]. This valence distribution, however, is at odds with photoemission spectroscopy results for *Pbnm* $BiNiO_3$ that reveal that the nickel valence is far from being Ni^{3+} [19].

The electronic properties of $BiNiO_3$ have recently been calculated using band-structure methods supplemented with the on-site Coulomb correlations for the Ni 3*d* states within density-functional theory (DFT)+*U* [21] and dynamical

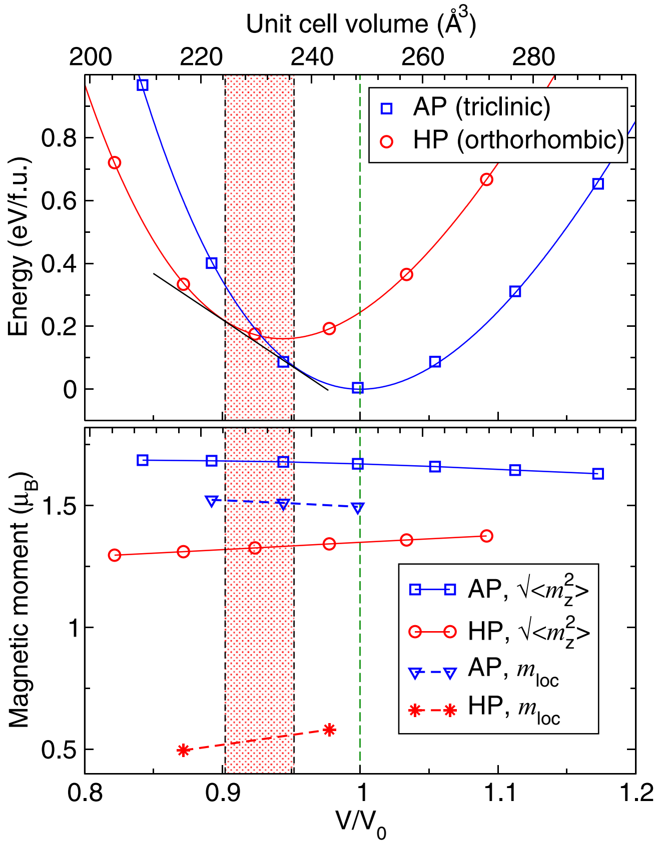

FIG. 1. Total energy (top) and local magnetic moments (bottom) of paramagnetic BiNiO$_3$ obtained by DFT+DMFT for the ambient-pressure $P\bar{1}$ (AP) and high-pressure *Pbnm* (HP) phases as a function of the unit cell volume at a temperature $T = 387$ K.

mean-field theory (DMFT) [22] methods [23]. However, these studies have mostly been focused on the valence skipping model, with a valence transition between the charge-ordered insulating [Bi$^{3+}_{0.5}$Bi$^{5+}_{0.5}$][Ni^{2+}] and the uniform metallic [Bi^{3+}][Ni^{3+}] state, assuming a long-range magnetic ordering. In fact, however, the MIT transition in BiNiO$_3$ is known to occur in the *paramagnetic* state, implying the importance of electronic correlations. Moreover, a recent electronic structure study of BiNiO$_3$ using DFT and slave rotor methods suggests that BiNiO$_3$ is a self-doped Mott insulator [24].

In this Rapid Communication, we explore the evolution of the electronic structure, magnetic state, and phase stability of paramagnetic BiNiO$_3$ near the pressure-induced Mott MIT. We employ a fully self-consistent in charge density DFT+DMFT approach [25] implemented with plane-wave pseudopotentials [26,27] which makes it possible to capture all generic aspects of the interplay between the electronic correlations, magnetic states, and crystal structure of BiNiO$_3$ near the Mott MIT [28]. The DFT+DMFT calculations explicitly include the Bi 6*s*, O 2*p*, and Ni 3*d* valence states, by constructing a basis set of atomic-centered Wannier functions within the energy window spanned by the *s*-*p*-*d* band complex [29]. This allows us to take into account a charge transfer between the Bi 6*s*, O 2*p*, and Ni 3*d* states, accompanied by the strong on-site Coulomb correlations of the Ni 3*d* electrons. We use the continuous-time hybridization-expansion (segment) quantum Monte Carlo algorithm in order to solve the realistic many-body problem [30]. We take the average Hubbard $U = 6$ eV and Hund's exchange $J = 0.95$ eV as estimated previously for *R*NiO$_3$ [7,9]. We use the fully localized double-counting correction, evaluated from the self-consistently determined local occupations, to account for the electronic interactions already described by DFT.

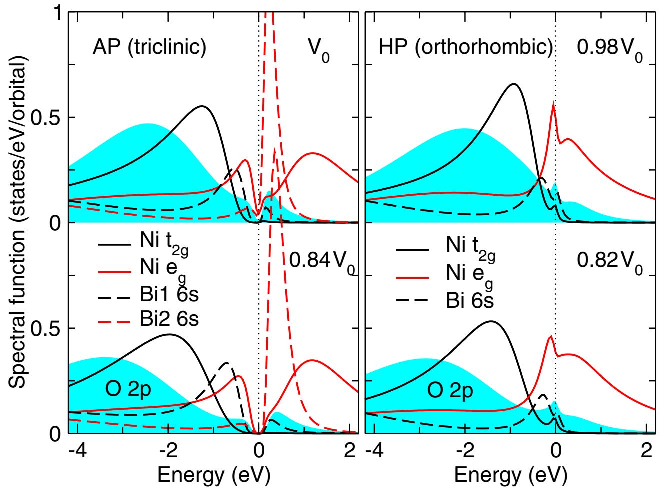

FIG. 2. Orbitally resolved spectral functions of BiNiO$_3$ calculated within DFT+DMFT using the maximum entropy method for the ambient-pressure $P\bar{1}$ (left panel) and high-pressure *Pbnm* (right panel) structures for different unit cell volumes at a temperature $T = 387$ K.

In Fig. 1 we display our DFT+DMFT results for the phase equilibrium and local magnetic moments of Ni ions of paramagnetic BiNiO$_3$. In these calculations, we adopt the crystal structure data for the ambient pressure triclinic $P\bar{1}$ and high-pressure orthorhombic *Pbnm* structures (taken at a pressure of ~7.7 GPa) from experiment [11], and evaluate the DFT+DMFT total energies as a function of lattice volume. Overall, our results for the electronic structure and lattice properties of BiNiO$_3$ agree well with experimental data [10–13,19]. In particular, the triclinic $P\bar{1}$ phase is found to be thermodynamically stable at ambient pressure, with a total-energy difference between the ambient-pressure and high-pressure phases of ~160 meV/f.u. The calculated equilibrium lattice volume $V_0 = 248.8$ Å^3 and bulk modulus $K_0 = 149$ GPa ($K' \equiv dK/dP$ is fixed to $K' = 4$). Interestingly, all the Ni sites (the insulating $P\bar{1}$ phase has four inequivalent Ni sites) are nearly equivalent and are in the Ni^{2+} state. The Ni^{2+} state is also confirmed by the eigenvalues analysis of the reduced Ni 3*d* density matrix, which suggests that the Ni ions are in the $\sqrt{0.63}|d^8\rangle + \sqrt{0.32}|d^9\rangle$ state (the rest of the contributions are below 0.05). Moreover, the calculated local (instantaneous) magnetic moment $\sqrt{\langle\hat{m}_z^2\rangle} \simeq 1.67\mu_B$ agrees with the high-spin $S = 1$ state of the Ni^{2+} ions.

Our calculations for the insulating $P\bar{1}$ phase of BiNiO$_3$ give a self-doped Mott insulator [31] with an energy gap of ~0.3 eV (see the left panel of Fig. 2), in agreement with the resistivity and photoemission experiments [10,19] (see also Supplemental Material Fig. S3). In particular, the energy gap lies between the occupied and unoccupied Ni e_g states, strongly mixed with the O $2p$ and the empty Bi2 $6s$ states (the Bi1 $6s$ states are fully occupied). The O $2p$ states are about -3.6 eV below the Fermi level, but have a substantial contribution both above and below E_F. The latter is due to the strongly covalent B $6s$–O $2p$ bonding, suggesting creation of a ligand hole caused by a charge transfer between Bi $6s$ and O $2p$. While the occupied Bi1 and Bi2 $6s$ states are seen to be localized deep below E_F, at about -10 eV, the empty Bi2 $6s$ states appear right at the bottom of the conduction band, with a sharp resonant peak at $\sim$0.4 eV. The top of the valence band has a mixed Ni $3d$ and O $2p$ character, with a resonant peak in the filled e_g bands located at about -0.4 eV below the Fermi level, which can be ascribed to the formation of a Zhang-Rice bound state [32].

Our result for the insulating $P\bar{1}$ phase is characterized by a remarkable charge disproportionation of the Bi $6s$ states (due to the appearance of two different Bi sites with sufficiently different oxygen environment in the insulating phase). In fact, while the Bi1 $6s$ states are almost completely occupied, the Bi2 $6s$ Wannier occupancy is only about 1.56. This implies a charge difference of $\Delta N_{\text{Bi-}6s} \sim 0.42$, i.e., it is about 21% of the ideal Bi^{3+}-Bi^{5+} value. Interestingly, the corresponding Bi $6s$ charge difference is in agreement with a charge disproportionation of $\sim$0.2 (i.e., of $\sim$20% of the ideal valence skipping) found in the low-temperature charge-ordered phases of the mixed-valent oxides, such as Fe_3O_4 [33], and of $\sim$0.2–0.3 charge disproportionation of the Ni ions in $R\text{NiO}_3$ [5]. Moreover, previous estimates for the bond-disproportionated insulating phases of the bismuth perovskites BaBiO_3 and SrBiO_3 show a small charge disproportionation between the Bi ions of $\sim$0.3 [34]. We also verified our result for $\Delta N_{\text{Bi-}6s}$ by calculating the corresponding charge difference within the Bi-ion radius of 1.31 Å, a typical value for the Bi^{3+} ion. Nevertheless, we find that the result is robust, with $\Delta N_{\text{Bi-}6s} \sim 0.34$. While all the Ni's are in the Ni^{2+} state (and, as we will show below, the Ni^{2+} state remains stable above the MIT in the metallic *Pbnm* phase) this suggests the stabilization of the charge-disproportionated $\text{Bi1}^{3+}_{0.5}(\text{Bi2}^{(3+\delta)+}\underline{L}^{2-\delta})_{0.5}$ valence configuration in the insulating $P\bar{1}$ phase of BiNiO_3. We argue that the obtained valence configuration can be rationalized as being intermediate between the two limits: the pure valence skipping Bi^{3+}-Bi^{5+} and the Bi-O bond disproportionation Bi^{3+}-[Bi$^{3+}\underline{L}^2$] models.

Interestingly, the energy gap of the triclinic BiNiO_3 phase is seen to increase upon (a uniform) compression (while decreasing and even closing upon expansion) of the unit cell volume (see the lower panel of Fig. 2). This counterintuitive change of the energy gap value in a Mott insulator is accompanied by a remarkable increase of charge disproportionation of the Bi ions (under pressure), suggesting the importance of a Bi $6s$-O $2p$ charge transfer. In particular, our results show that the Bi $6s$ charge disproportionation becomes larger in the $P\bar{1}$ crystal structure of BiNiO_3 upon decrease of the lattice volume (see Fig. 3). Upon compression, the Bi2 $6s$ orbital occupation gradually decreases, whereas the Bi1 $6s$ states are fully occupied, with a nearly constant occupation $N_{\text{Bi1-}6s} \sim 1.97$. In addition, our DFT+DMFT calculations using different Hubbard U values ($U = 5$ eV and 8 eV) show that the energy gap increases upon increasing of U, in agreement with the behavior of a Mott insulator. Interestingly, the Bi $6s$ charge disproportionation becomes larger for the larger U values, by $\sim$5% upon increasing of the U value from $U = 6$ to 8 eV.

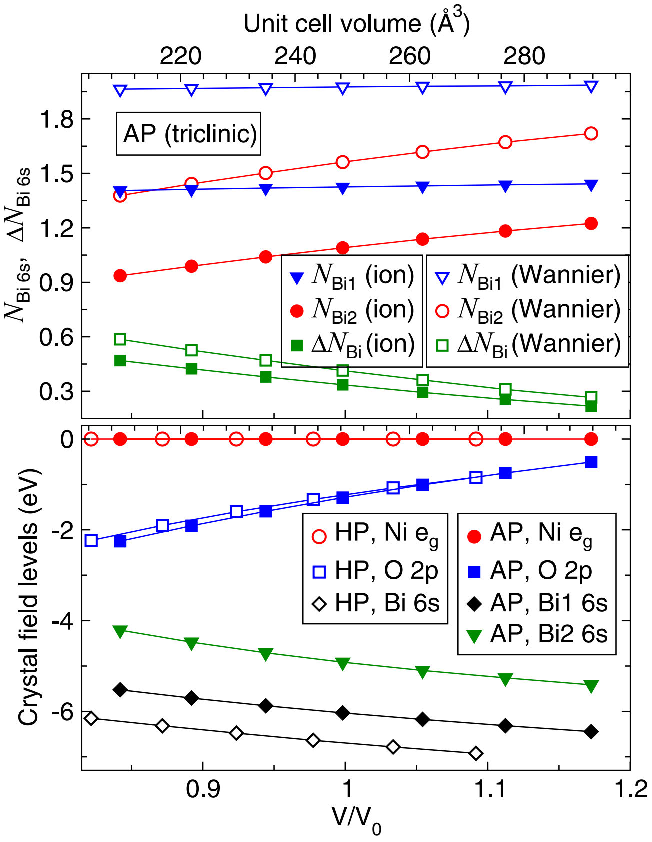

FIG. 3. Bi $6s$ occupations for the ambient-pressure (AP) $P\bar{1}$ phase of BiNiO_3 calculated by DFT+DMFT as a function of lattice volume (top). ΔN_{Bi} denotes the corresponding Bi $6s$ charge disproportionation ($\Delta N_{\text{Bi}} = N_{\text{Bi1}} - N_{\text{Bi2}}$). Bottom: the Ni e_g and O $2p$ crystal field levels for the AP and high-pressure *Pbnm* BiNiO_3 [35].

This behavior is consistent with the change of the crystal field levels of the Ni e_g, O $2p$, and Bi $6s$ states under pressure (see Fig. 3). In fact, the O $2p$ levels are found to shift deep below the Ni e_g states under pressure, whereas the Bi $6s$ states go up in energy. The change of the O $2p$ and Bi $6s$ crystal field levels leads to the enhancement of the Bi $6s$-O $2p$ hybridization under pressure, supporting the hybridization-switching mechanism proposed by Paul *et al.* [24]. Our results suggest that the $P\bar{1}$-structured BiNiO_3 is an *unconventional* Mott insulator in which the correlated insulating state is in much respect controlled by an s-p level splitting between the uncorrelated A-site Bi $6s$ and ligand O $2p$ states.

Upon further compression the $P\bar{1}$-structured BiNiO_3 becomes metallic below $\sim 0.5V_0$, with the (instantaneous) local moment of $\sim$1.36μ_B. The MIT is accompanied with a collapse of local moments due to delocalization of the Ni $3d$ electrons, as seen from the behavior of local spin susceptibility $\chi(\tau) = \langle \hat{m}_z(\tau)\hat{m}_z(0)\rangle$ (see Fig. 4). In fact, $\chi(\tau)$ is seen to decay fast with the imaginary time τ. In agreement with this, the fluctuating moment is only of $\sim$0.75μ_B (evaluated as $m_{\text{loc}} = [T\int_0^{1/T}\chi(\tau)d\tau]^{1/2}$), which differs sufficiently from

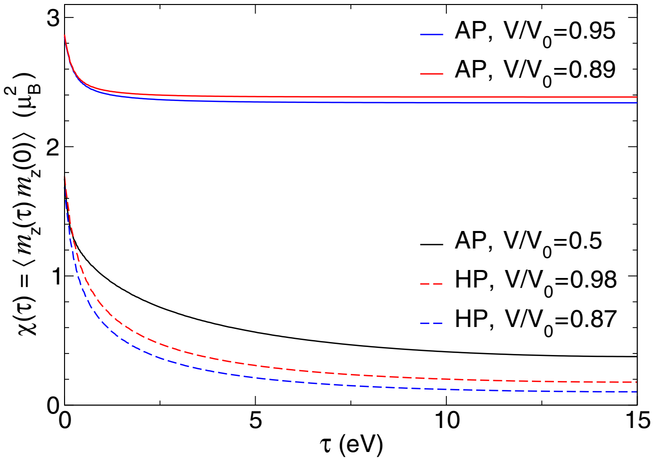

FIG. 4. Local spin correlation function $\chi(\tau) = \langle \hat{m}_z(\tau)\hat{m}_z(0)\rangle$ of the Ni $3d$ states calculated by DFT+DMFT for the ambient-pressure $P\bar{1}$ (AP) and the high-pressure $Pbnm$ (HP) structures of $BiNiO_3$ for different volumes.

the instantaneous moment. While the Bi $6s$ charge disproportionation is large in the highly compressed metallic $P\bar{1}$ phase, $\Delta N_{\text{Bi-}6s} \sim 1.04$, this suggests that the Bi $6s$ charge ordering alone cannot explain the insulating state of $BiNiO_3$. In agreement with this, our results for structural optimization of the $P\bar{1}$ phase within nonmagnetic DFT give a metal with no evidence for the Bi $6s$ charge disproportionation (all the Bi sites are found to have nearly the same oxygen environment), implying the crucial importance of strong localization of the Ni $3d$ electrons due to correlation effects [3].

Most importantly, our DFT+DMFT results provide clear evidence that $BiNiO_3$ undergoes a structural transition from the triclinic insulating $P\bar{1}$ to orthorhombic metallic $Pbnm$ structure below $\sim 0.95V_0$ (above 8 GPa), in agreement with experiment [11–13]. We found that the transition pressure depends very sensitively on the choice of the Hubbard U value, with $P_c \simeq 1$ and 15 GPa for $U = 5$ and 8 eV, respectively. The calculated bulk modulus ($U = 6$ eV) is $K_0 \sim 143$ GPa, i.e., K_0 is found to decrease by ~4% upon the MIT into the metallic state. The latter is rather uncommon for a Mott MIT, indicating the importance of lattice effects at the MIT in $BiNiO_3$ [3].

The $Pbnm$ phase of $BiNiO_3$ is a correlated metal, characterized by a Fermi-liquid-like behavior with a weak damping of quasiparticles at the Fermi energy and by a substantial mass renormalization of $\frac{m^*}{m} \sim 2.5$ of the Ni e_g bands. The Ni e_g states show a quasiparticle peak at the Fermi level, with the upper Hubbard band at ~1.0 eV (see Fig. 2 and Supplemental Material Fig. S3). The calculated Ni-ion local magnetic moment of $1.3\mu_B$ differs sufficiently from the fluctuating one $\sim 0.5\mu_B$, implying delocalization of the Ni $3d$ electrons at the transition. Indeed, our result for the local susceptibility shows itinerant-moment-like behavior, similar to that of the highly pressurized $P\bar{1}$ phase (see Fig. 4). The $Pbnm$ phase is found to be metallic for all unit cell volumes studied here, as well as even for a large Hubbard $U = 12$ eV. The pressure-induced MIT is found to be accompanied by a collapse of the lattice volume by $\sim 5.2\%$, resulting in the melting of charge disproportionation of the Bi sites. Thus, in the $Pbnm$ phase all the Bi sites are equivalent, whereas the Bi $6s$ states are fully occupied, i.e., Bi^{3+}. Moreover, our analysis of eigenvalues of the reduced Ni $3d$ density matrix suggests that the Ni sites are in a Ni^{2+} state, with an atomic configuration $\simeq \sqrt{0.56}|d^8\rangle + \sqrt{0.30}|d^9\rangle$. We also notice a minor, below ~10%, contribution due to the d^7 atomic state, $\sqrt{0.09}|d^7\rangle$. Based on this result, we conclude that no change of the valence state of the Ni^{2+} ions occurs across the pressure-induced MIT in $BiNiO_3$, i.e., the Ni^{2+} state remains stable. The latter is in sharp contrast with the valence skipping Bi/Ni model proposed earlier for $BiNiO_3$ [11,20]. Our results suggest a microscopic mechanism of a Mott MIT under pressure which is controlled by a charge transfer between the A-site Bi $6s$ and ligand O $2p$ states. The pressure-induced MIT in $BiNiO_3$ is accompanied by a transition from the charge-disproportionated $\text{Bi1}^{3+}_{0.5}(\text{Bi2}^{(3+\delta)+}\underline{L}^{2-\delta})_{0.5}$ to the charge-uniform $Bi^{3+}\underline{L}^2$ valence state. The Bi $6s$ charge disproportionation (in the insulating $P\bar{1}$ phase) occurs together with the MIT, which follows rather than produces the structural transition. We therefore conclude that the pressure-induced MIT and the concomitant melting of the Bi $6s$ charge ordering in $BiNiO_3$ is driven by the crystal structure transition. The latter highlights the complex interplay between the electronic structure and lattice effects in the vicinity of a Mott MIT in $RNiO_3$ nickelates [3].

In conclusion, we employed the DFT+DMFT approach to determine the electronic structure and phase stability of paramagnetic $BiNiO_3$ across the pressure-induced Mott MIT. Our results for the $P\bar{1}$-structured $BiNiO_3$ under pressure propose a mechanism for a correlation-driven metal-insulator transition, in which the Mott insulating state is (in much respect) controlled by the s-p level splitting between the uncorrelated A-site Bi $6s$ and ligand O $2p$ states. We show that the pressure-induced MIT in $BiNiO_3$ is associated with the melting of charge disproportionation of the Bi ions and is accompanied by delocalization of the Ni $3d$ electrons. The phase transition results in a charge transfer between the Bi $6s$ and O $2p$ states, while the Ni sites remain to be Ni^{2+}. Our results suggest that the pressure-induced change of the crystal structure drives the MIT in $BiNiO_3$. We argue that the $RNiO_3$ compounds (with $R =$ rare earth and Bi) obey an intrinsic instability driven by the interplay of electron correlations and lattice effects, depending on the R-ion radius. It is associated with a crossover from charge disproportionation of the perovskite B-site Ni ions (realized for the R ions with the ionic radii smaller than that of La) to that of the A-site R ions (for large R ions), with $LaNiO_3$ being in between.

We thank O. Peil for valuable discussions. We acknowledge the support from Russian Foundation for Basic Research (Project No. 18-32-20076).The DFT calculations were supported by the Ministry of Science and Higher Education of the Russian Federation (theme “Electron” No. AAAA-A18-118020190098-5).

[1] M. Imada, A. Fujimori, and Y. Tokura, Rev. Mod. Phys. **70**, 1039 (1998).

[2] S. Middey, J. Chakhalian, P. Mahadevan, J. W. Freeland, A. J. Millis, and D. D. Sarma, Annu. Rev. Mater. Res. **46**, 305 (2016); S. Catalano, M. Gibert, J. Fowlie, J. Íñiguez, J.-M. Triscone, and J. Kreisel, Rep. Prog. Phys. **81**, 46501 (2018).

[3] A. Subedi, O. E. Peil, and A. Georges, Phys. Rev. B **91**, 075128 (2015); A. B. Georgescu, O. E. Peil, A. S. Disa, A. Georges, and A. J. Millis, Proc. Natl. Acad. Sci. **116**, 14434 (2019); O. E. Peil, A. Hampel, C. Ederer, and A. Georges, Phys. Rev. B **99**, 245127 (2019).

[4] A. Mercy, J. Bieder, J. Íñiguez, and Ph. Ghosez, Nat. Commun. **8**, 1677 (2017).

[5] J. B. Torrance, P. Lacorre, A. I. Nazzal, E. J. Ansaldo, and Ch. Niedermayer, Phys. Rev. B **45**, 8209(R) (1992); J. L. García-Muñoz, J. Rodríguez-Carvajal, P. Lacorre, and J. B. Torrance, *ibid.* **46**, 4414 (1992); J. A. Alonso, J. L. García-Muñoz, M. T. Fernández-Díaz, M. A. G. Aranda, M. J. Martínez-Lope, and M. T. Casais, Phys. Rev. Lett. **82**, 3871 (1999); G. Catalan, Phase Transit. **81**, 729 (2008); J. L. García-Muñoz, M. A. G. Aranda, J. A. Alonso, and M. J. Martínez-Lope, Phys. Rev. B **79**, 134432 (2009).

[6] M. Medarde, C. Dallera, M. Grioni, B. Delley, F. Vernay, J. Mesot, M. Sikora, J. A. Alonso, and M. J. Martínez-Lope, Phys. Rev. B **80**, 245105 (2009).

[7] H. Park, A. J. Millis, and C. A. Marianetti, Phys. Rev. Lett. **109**, 156402 (2012); Phys. Rev. B **89**, 245133 (2014); **90**, 235103 (2014); A. Hampel and C. Ederer, *ibid.* **96**, 165130 (2017); A. Hampel, P. Liu, C. Franchini, and C. Ederer, npj Quant. Mater. **4**, 5 (2019).

[8] S. Johnston, A. Mukherjee, I. Elfimov, M. Berciu, and G. A. Sawatzky, Phys. Rev. Lett. **112**, 106404 (2014); J. Varignon, M. N. Grisolia, J. Íñiguez, A. Barthélémy, M. Bibes, npj Quant. Mater. **2**, 21 (2017).

[9] E. A. Nowadnick, J. P. Ruf, H. Park, P. D. C. King, D. G. Schlom, K. M. Shen, and A. J. Millis, Phys. Rev. B **92**, 245109 (2015).

[10] S. Ishiwata, M. Azuma, M. Takano, E. Nishibori, M. Takata, M. Sakatac, and K. Kato, J. Mater. Chem. **12**, 3733 (2002).

[11] M. Azuma, S. Carlsson, J. Rodgers, M. G. Tucker, M. Tsujimoto, S. Ishiwata, S. Isoda, Y. Shimakawa, M. Takano, and J. P. Attfield, J. Am. Chem. Soc. **129**, 14433 (2007).

[12] S. J. E. Carlsson, M. Azuma, Y. Shimakawa, M. Takano, A. Hewat, and J. P. Attfield, J. Solid State Chem. **181**, 611 (2008).

[13] M. Azuma, W. Chen, H. Seki, M. Czapski, O. Smirnova, O. Kengo, M. Mizumaki, T. Watanuki, N. Ishimatsu, N. Kawamura *et al.*, Nat. Commun. **2**, 347 (2011); K. Oka, M. Mizumaki, Ch. Sakaguchi, A. Sinclair, C. Ritter, J. P. Attfield, and M. Azuma, Phys. Rev. B **88**, 014112 (2013).

[14] See Supplemental Material at http://link.aps.org/supplemental/10.1103/PhysRevB.100.161112 for a detailed discussion of the electronic structure and lattice properties of BiNiO$_3$ near the MIT.

[15] K. Momma and F. Izumi, J. Appl. Crystallogr. **44**, 1272 (2011).

[16] Interestingly, the insulating RNiO$_3$ phases also exhibit a complex (noncollinear) antiferromagnetic order below T_{N}, but with an uncommon wave vector $\mathbf{q} = (\frac{1}{2}, 0, \frac{1}{2})$.

[17] It is also interesting to point out that magnetic ordering is present only in the insulating triclinic phase. The metallic orthorhombic phase was found to be nonmagnetic down to 10 K [13].

[18] S. Ishiwata, M. Azuma, M. Hanawa, Y. Moritomo, Y. Ohishi, K. Kato, M. Takata, E. Nishibori, M. Sakata, I. Terasaki *et al.*, Phys. Rev. B **72**, 045104 (2005).

[19] H. Wadati, M. Takizawa, T. T. Tran, K. Tanaka, T. Mizokawa, A. Fujimori, A. Chikamatsu, H. Kumigashira, M. Oshima, S. Ishiwata *et al.*, Phys. Rev. B **72**, 155103 (2005).

[20] M. Mizumaki, N. Ishimatsu, N. Kawamura, M. Azuma, Y. Shimakawa, M. Takano, and T. Uozumi, Phys. Rev. B **80**, 233104 (2009).

[21] V. I. Anisimov, J. Zaanen, and O. K. Andersen, Phys. Rev. B **44**, 943 (1991).

[22] W. Metzner and D. Vollhardt, Phys. Rev. Lett. **62**, 324 (1989); A. Georges, G. Kotliar, W. Krauth, and M. J. Rozenberg, Rev. Mod. Phys. **68**, 13 (1996); V. I. Anisimov, A. I. Poteryaev, M. A. Korotin, A. O. Anokhin, and G. Kotliar, J. Phys.: Condens. Matter **9**, 7359 (1997); G. Kotliar, S. Y. Savrasov, K. Haule, V. S. Oudovenko, O. Parcollet, and C. A. Marianetti, Rev. Mod. Phys. **78**, 865 (2006); J. Kuneš, I. Leonov, P. Augustinský, V. Křápek, M. Kollar, and D. Vollhardt, Eur. Phys. J.: Spec. Top. **226**, 2641 (2017).

[23] M. Q. Cai, G. W. Yang, X. Tan, Y. L. Cao, L. L. Wang, W. Y. Hu, and Y. G. Wang, Appl. Phys. Lett. **91**, 101901 (2007); J. A. McLeod, Z. V. Pchelkina, L. D. Finkelstein, E. Z. Kurmaev, R. G. Wilks, A. Moewes, I. V. Solovyev, A. A. Belik, and E. Takayama-Muromachi, Phys. Rev. B **81**, 144103 (2010); S. Kojima, J. Nasu, and A. Koga, *ibid.* **94**, 045103 (2016); M. Naka, H. Seo, and Y. Motome, Phys. Rev. Lett. **116**, 056402 (2016); M. Pugaczowa-Michalska and J. Kaczkowski, Comput. Mater. Sci. **126**, 407 (2017); Y. Liu, Z. Wang, D. Chang, Q. Sun, M. Chao, and Y. Jia, *ibid.* **113**, 198 (2016).

[24] A. Paul, A. Mukherjee, I. Dasgupta, A. Paramekanti, and T. Saha-Dasgupta, Phys. Rev. Lett. **122**, 016404 (2019).

[25] K. Haule, Phys. Rev. B **75**, 155113 (2007); L. V. Pourovskii, B. Amadon, S. Biermann, and A. Georges, *ibid.* **76**, 235101 (2007); B. Amadon, F. Lechermann, A. Georges, F. Jollet, T. O. Wehling, and A. I. Lichtenstein, *ibid.* **77**, 205112 (2008); M. Aichhorn, L. Pourovskii, V. Vildosola, M. Ferrero, O. Parcollet, T. Miyake, A. Georges, and S. Biermann, *ibid.* **80**, 085101 (2009).

[26] S. Baroni, S. de Gironcoli, A. Dal Corso, and P. Giannozzi, Rev. Mod. Phys. **73**, 515 (2001); P. Giannozzi, S. Baroni, N. Bonini, M. Calandra, R. Car, C. Cavazzoni, D. Ceresoli, G. L. Chiarotti, M. Cococcioni, I. Dabo *et al.*, J. Phys.: Condens. Matter **21**, 395502 (2009).

[27] I. Leonov, N. Binggeli, Dm. Korotin, V. I. Anisimov, N. Stojić, and D. Vollhardt, Phys. Rev. Lett. **101**, 096405 (2008); I. Leonov, Dm. Korotin, N. Binggeli, V. I. Anisimov, and D. Vollhardt, Phys. Rev. B **81**, 075109 (2010).

[28] M. Aichhorn, S. Biermann, T. Miyake, A. Georges, and M. Imada, Phys. Rev. B **82**, 064504 (2010); O. E. Peil, A. Georges, and F. Lechermann, Phys. Rev. Lett. **107**, 236404 (2011); K. Ohta, R. E. Cohen, K. Hirose, K. Haule, K. Shimizu, and Y. Ohishi, *ibid.* **108**, 026403 (2012); D. Grieger, Ch. Piefke, O. E. Peil, and F. Lechermann, Phys. Rev. B **86**, 155121 (2012); I. Leonov, V. I. Anisimov, and D. Vollhardt, *ibid.* **91**, 195115 (2015); I. Leonov, *ibid.* **92**, 085142 (2015); A. O. Shorikov, A. V. Lukoyanov, V. I. Anisimov, and S. Y. Savrasov, *ibid.* **92**, 035125 (2015); I. Leonov, S. L. Skornyakov, V. I. Anisimov,

and D. Vollhardt, Phys. Rev. Lett. **115**, 106402 (2015); I. Leonov, L. Pourovskii, A. Georges, and I. A. Abrikosov, Phys. Rev. B **94**, 155135 (2016); F. Lechermann, N. Bernstein, I. I. Mazin, and R. Valenti, Phys. Rev. Lett. **121**, 106401 (2018); E. Greenberg, I. Leonov, S. Layek, Z. Konopkova, M. P. Pasternak, L. Dubrovinsky, R. Jeanloz, I. A. Abrikosov, and G. Kh. Rozenberg, Phys. Rev. X **8**, 031059 (2018); I. Leonov, G. Kh. Rozenberg, and I. A. Abrikosov, npj Comput. Mater. **5**, 90 (2019).

[29] N. Marzari, A. A. Mostofi, J. R. Yates, I. Souza, and D. Vanderbilt, Rev. Mod. Phys. **84**, 1419 (2012); V. I. Anisimov, D. E. Kondakov, A. V. Kozhevnikov, I. A. Nekrasov, Z. V. Pchelkina, J. W. Allen, S.-K. Mo, H.-D. Kim, P. Metcalf, S. Suga *et al.*, Phys. Rev. B **71**, 125119 (2005); Dm. Korotin, A. V. Kozhevnikov, S. L. Skornyakov, I. Leonov, N. Binggeli, V. I. Anisimov, and G. Trimarchi, Eur. Phys. J. B **65**, 91 (2008); G. Trimarchi, I. Leonov, N. Binggeli, Dm. Korotin, and V. I. Anisimov, J. Phys.: Condens. Matter **20**, 135227 (2008).

[30] E. Gull, A. J. Millis, A. I. Lichtenstein, A. N. Rubtsov, M. Troyer, and P. Werner, Rev. Mod. Phys. **83**, 349 (2011).

[31] J. Zaanen, G. A. Sawatzky, and J. W. Allen, Phys. Rev. Lett. **55**, 418 (1985); M. A. Korotin, V. I. Anisimov, and D. I. Khomskii, and G. A. Sawatzky, *ibid.* **80**, 4305 (1998).

[32] F. C. Zhang and T. M. Rice, Phys. Rev. B **37**, 3759(R) (1988).

[33] J. P. Wright, J. P. Attfield, and P. G. Radaelli, Phys. Rev. B **66**, 214422 (2002); I. Leonov, A. N. Yaresko, V. N. Antonov, and V. I. Anisimov, *ibid.* **74**, 165117 (2006); H.-T. Jeng, G. Y. Guo, and D. J. Huang, *ibid.* **74**, 195115 (2006); M. S. Senn, J. P. Wright, and J. P. Attfield, Nature (London) **481**, 173 (2012); N. Pontius, T. Kachel, C. Schüßler-Langeheine, W. F. Schlotter, M. Beye, F. Sorgenfrei, C. F. Chang, A. Föhlisch, W. Wurth, P. Metcalf *et al.*, Appl. Phys. Lett. **98**, 182504 (2011); G. Perversi, E. Pachoud, J. Cumby, J. M. Hudspeth, J. P. Wright, S. A. J. Kimber, and J. P. Attfield, Nat. Commun. **10**, 2857 (2019).

[34] K. Foyevtsova, A. Khazraie, I. Elfimov, and G. A. Sawatzky, Phys. Rev. B **91**, 121114(R) (2015); N. C. Plumb, D. J. Gawryluk, Y. Wang, Z. Ristić, J. Park, B. Q. Lv, Z. Wang, C. E. Matt, N. Xu, T. Shang *et al.*, Phys. Rev. Lett. **117**, 037002 (2016); A. Khazraie, K. Foyevtsova, and I. Elfimov, and G. A. Sawatzky, Phys. Rev. B **98**, 205104 (2018).

[35] The crystal field levels for the Ni e_g states taken here as a reference energy are evaluated from the first moments of the interacting lattice Green's function as $\Delta_{\mathrm{cf}} \equiv \mathrm{diag}[\Sigma_{\mathbf{k}} H^{\mathrm{DFT}}(\mathbf{k}) + \mathrm{Re}\Sigma(i\omega_n \to \infty)]$. Here, $H^{\mathrm{DFT}}(\mathbf{k})$ is the effective low-energy *s*-*p*-*d* Hamiltonian in the Wannier basis set. $\Sigma(i\omega_n \to \infty)$ is a static Hartree contribution from self-energy $\Sigma(i\omega_n)$.